ISSN 1811-2382, Polymer Science, Series C, 2018, Vol. 60, Suppl. 1, pp. S84–S94. © Pleiades Publishing, Ltd., 2018.
Original Russian Text © L.I. Klushin, A.M. Skvortsov, S. Qi, F. Schmid, 2018, published in Vysokomolekulyarnye Soedineniya, Seriya C, 2018, Vol. 60, No. 2, pp. 181–192.

Polydisperse Brush with the Linear Density Profile

L. I. Klushin[a,b], A. M. Skvortsov[c,*], S. Qi[d], and F. Schmid[d]

[a] *Institute of Macromolecular Compounds, Russian Academy of Sciences, St. Petersburg, 199004 Russia*
[b] *Department of Physics, American University of Beirut, P. O. Box 11-0236, Beirut, 1107 2020 Lebanon*
[c] *St. Petersburg State Chemical and Pharmaceutical Academy, St. Petersburg, 197022 Russia*
[d] *Institut für Physik, Johannes Gutenberg-Universität, Mainz Staudingerweg 7, Mainz, D-55099 Germany*
**e-mail: astarling@yandex.ru*

Received March 19, 2018

Abstract—Macromolecules densely end-grafted to a planar solid surface form a polymer monolayer (brush). It is known that, in a good solvent, the density profile of monodisperse brushes parabolically decays on moving away from the plane. Using the analytical theory and computer simulation methods, we studied the structure of a polydisperse brush from homopolymers, for which molecular-mass distribution is set by the Schulz–Zimm distribution. It is found that, at a polydispersity index of 1.143, the polymer brush in a good solvent has a linear density profile. In this brush, the average distance of chain ends to the grafting plane is proportional to the square of their contour length. If any chain of the brush is chemically modified so that it will be able to adsorb on the grafting surface, then the adsorption of this chain inside the brush will proceed via a discontinuous first-order phase transition with the bimodal distribution of the order parameter (free end height). This transition has unusual features: the energy of adsorption corresponding to the midpoint of the transition is proportional to the contour length of the adsorbing chain N, the sharpness of the transition is proportional to N^2, and the height of the barrier separating adsorbed and desorbed states is proportional to N^3. The predicted dependences are verified by computer simulation.

DOI: 10.1134/S1811238218020121

INTRODUCTION

Polymer chains densely end-grafted to a planar inert solid surface are called a polymer monolayer or brush. For neighboring chains to overlap, the grafting density should be fairly high. Polymer brushes have long been used for the surface modification of various objects. This phenomenon made it possible to increase the protector and antipollution properties of biomaterials [1, 2], found wide use in biomedicine [3], improved tribological characteristics and reduced friction in machines [4, 5] and in the prosthetics of artificial joints [6], and enabled the synthesis of smart surfaces with stimuli-responsive mechanical and optical characteristics [7]. At present, the use of polymer brushes has formed a separate field of nanotechnologies [8, 9]. In our opinion, the rapid progress in this field is in many respects is associated with the fact that, already at early stages, the detailed theoretical description of the structure of polymer brushes was obtained which provided the possibility to evaluate and predict their potential.

Polymer brushes have been the subject of extensive theoretical study for more than three decades since publication of the theoretical work by S. Alexander [10], in which expression for the average thickness of the monodisperse brush $H \sim N\sigma^{1/3}$ was derived in terms of the mean-field approach. In the Alexander theory, the density profile of the brush was supposed to be constant, except the near-wall region of order $\xi \sim \sigma^{-1/2}$. The first calculations of brushes in a good solvent by the self-consistent field method were performed in 1988 [11, 12]. It was shown that, as opposed to predictions from the mean field theory, in the central region of the brush, the density profile decays parabolically on moving away from the grafting plane, while in the monolayer decoration it decays exponentially. Another unexpected point was abnormally high fluctuations of brush free ends—they extended to distances on the order of H, that is, the whole thickness of the monolayer.

The results of these calculations induced E.B. Zhulina, O.V. Borisov, and V.A Pryamistin to develop the first analytical self-consistent field theory of monodisperse brushes immersed in a good solvent [13, 14], which agrees well with numerical calculations [11, 12]. Remarkably, simultaneously and quite independently, American researchers S.T. Milner, T.A. Witten, and M. Cates advanced the analogous theory of monodisperse polymer brushes with a parabolic density profile [15, 16]. The mathematical apparatus of these two theories was drastically different; however, their outcomes coincided. It is interesting that the Milner–

Witten–Cates theory was also triggered by numerical calculations [17], although comparison between them was absent.

Currently, there is a large body of theoretical data describing structural features of monodisperse polymer brushes coating solid surfaces of different shapes and taking into account the quality of solvent and the thermodynamic flexibility of grafted macromolecules [18–24]. In addition, the behavior of a pair of monodisperse brushes upon their compression and interpenetration was studied [25–28]. The specific feature of the theoretical data on polymer brushes is not only the abundant information accumulated by computer simulation but also the existence of well-developed and approved analytical theories. Russian researchers E.B. Zhulina, O.V. Borisov, and T.M. Birshtein greatly contributed to the emergence and development of analytical theories (review [22]).

Note that in principle the possibility of constructing analytical theories of polymer brushes of different shape is determined by the existence of a self-consistent parabolic potential in brushes which, at not too high a grafting density, is universal and is preserved both for brushes consisting of linear chains and for brushes composed of star-shaped macromolecules or dendrons [29, 30]. This universal character is related to the monodisperse character of brushes; it disappears once polydispersity effects become operative. Just this circumstance is responsible for the fact that the overwhelming minority of analytical theories concerned monodisperse brushes solely.

In experiments to create monodisperse polymer brushes or brushes with a narrow molecular-mass distribution, well-fractionated polymer chains with the known average number of units N_n are grafted to the solid surface or are anchored to it. Given this procedure, grafted chains should diffuse and go through already formed brush parts; therefore, long and dense brushes cannot be synthesized. For this synthesis procedure, the maximum grafting density is approximately one chain per square nanometer [31]. Denser brushes are prepared using another procedure, according to which initiators are placed on the surface and grafted chains are polymerized from melt or solution. The resulting brushes turn out to be polydisperse, and, as was shown in [32], their chain length distribution is close to the Schulz–Zimm distribution and the polydispersity index is in the range of 1.1–1.2 regardless of polymerization time. Brushes with a wider distribution are typical of biological objects, for example, glycocalix coating the cells or the surface of blood vessels [33].

It is known that polydispersity strongly affects the properties of brushes, for example, the pressure–distance relationship changes during compression of two brushes [19, 34, 35]. The effect of polydispersity on the structure of polymer brushes was studied via self-consistent field numerical calculations [36] and analytical methods and computer simulation [37]. It was shown that, with increasing polydispersity, the brush thickness grows and the density profile changes and acquires a concave shape. Large fluctuations of the height of chain free ends above the grafting plane inherent in monodisperse brushes are suppressed by even a small polydispersity [37].

In this study, we will consider the planar surface coating polymer brush with a certain polydispersity at which the density profile has a strictly linear shape and, hence, creates inside the brush a self-consistent field with a linearly decreasing potential on moving away from the grafting plane. We will describe structural characteristics of chains of such a brush in a good solvent. Comparing characteristics of polydisperse and monodisperse brushes, we will examine behavior of the "probe" chain in these brushes. The probe chain will imply chain of a brush that differs from minority chains in its particular characteristic. For example, for the monodisperse brush the chain of another contour length may be probe. The probe chain which randomly mixed with minority chains of the brush may be of another chemical nature. We will suppose that another chemical nature of the probe chain makes itself evident as the only difference from minority chains, namely, it possesses sorption activity and may occur in the adsorbed state on the solid surface (on the grafting surface). The addition of desorbing agent to solution has no effect on the properties of minority chains of the brush but entails desorption of the probe chain. We will analyze influence of the internal self-consistent field of the brush on the character and features of probe chain switching from the adsorbed state to the stretched one. Predictions from the analytical theory will be verified by computer simulation. Gaining insight into behavior of probe chains inside polymer brushes is not only of academic interest, because modified chains specially included in the brush may be used as stimuli-responsive switches [38]. The possible coexistence of chemically different chains in the same solvent at different sorption activity of chains will be discussed at the end of the paper.

MODEL AND METHOD

In most Monte Carlo simulations of polymer brushes, the model of lattice or off-lattice flexible chain in a good solvent was used. Lattice chains had a fixed length, and in off-lattice chains, the number of units was fixed so that chains possessed finite extensibility. In our calculations a polymer chain is composed of beads, which are linked by elastic bonds (harmonic springs) with spring constant $\frac{3kT}{2a^2}$, where a is the average bond length, k is the Boltzmann constant, and T is temperature. Thus, in the used model, the polymer chain had infinite extensibility. The grafting point was located at distance z_0, assuming $0 < z_0 < a$.

In what follows, we will use kT as the energy unit and a as the length unit. Therefore, the length of any brush chain will simply coincide with its degree of polymerization N and the grafting density σ; that is, the number of chains per surface unit will be a dimensionless value as are the coordinate of chain free end height z and brush thickness H.

Another feature of the used model is that volume interactions between randomly approached units are taken into account. In Monte Carlo calculations, these interactions in the model off-lattice chains are usually considered by setting the potential of solid spheres; in lattice chains, by forbidding getting in neighboring cells. Volume interactions of units were taken into account approximately by calculating the local density of units φ around the chosen chain unit at distance b. The effective potential of volume interactions was specified as the product of excluded-volume parameter v and the squared local density φ^2 in the sphere of radius b. In calculations, we assume that $v = 1$, which corresponds to good solvent conditions. The described model was advanced in [39] and previously applied in [40]. The effect of radius b of local density averaging on the simulation results was analyzed in [40]. It was shown that at $b \geq 2$ the results of Monte Carlo simulation cease to be dependent on the choice of b.

Periodic boundary conditions were set along axes X and Y, and the impenetrable grafting plane was situated at $Z = 0$.

In calculation of polydisperse brushes, the distribution of chains was given as the Schulz–Zimm distribution [41, 42], which is most frequently used to describe polydispersity effects and corresponds to the synthesis of real brushes. This distribution is the two-parameter function of the number-average length of chains N_n and parameter k:

$$P(N) = \frac{k^k N^{k-1}}{\Gamma(k) N_n^k} \exp\left(-k \frac{N}{N_n}\right), \quad (1)$$

where $\Gamma(k)$ is a gamma function. Parameter k in the Schulz–Zimm distribution is related to the polydispersity index N_w/N_n via the relation

$$N_w/N_n = 1 + 1/k. \quad (2)$$

In the limit $k \to \infty$, the distribution transforms into a delta-shaped peak, and at $k = 1$, it becomes an exponentially decaying function. It is easy to verify that distribution $P(N)$ is normalized to unity. In this study, calculations are performed at the fixed number-average chain length $N_n = 100$.

In Monte Carlo simulations, as usual, the trial move was made to shift the chain unit to the new state at a distance comparable with the size of the chain length. Given this, the change in energy was calculated and the trial move was accepted or rejected according to the probability accepted in the Metropolis method. The first 4×10^5 steps per monomer were performed to equilibrate the system, and the next 4×10^5 steps were performed to extract average values. Averaging was performed over 48 MC simulation runs with different arrangement of grafted chains. The model and calculation method are described in more detail in [39, 40].

DENSITY PROFILES AND CHAIN SIZES IN MONODISPERSE AND POLYDISPERSE BRUSHES

Density Profiles

The density profile of monodisperse brushes is well studied and is described by the expression

$$\phi(z) = \phi_0\left(1 - \frac{z^2}{H_{mono}^2}\right) = \phi_0 - \frac{3\pi^2}{8}\frac{z^2}{N_n^2}, \quad (3)$$

where the density near the wall is

$$\phi_0 = \frac{3}{2}\left(\frac{\pi\sigma}{2}\right)^{2/3}, \quad (4)$$

and the thickness of the monodisperse brush is given by the known expression

$$H_{mono} = \left(\frac{4\sigma}{\pi^2}\right)^{1/3} N_n. \quad (5)$$

Hereinafter, σ is the grafting density and N_n is the number-average length of brush chains, which for the monodisperse brush is the same for all of the chains. Remember that monomer length a is assumed to be unity as the second virial coefficient v describing interaction between monomers inside the brush immersed in a good solvent, so that N, H, and σ are dimensionless quantities. The distribution of chain ends in the monodisperse brush is described by the known formula

$$P_{mono}(z) = \frac{3z}{H_{mono}^2}\left(1 - \frac{z^2}{H_{mono}^2}\right)^{1/2}. \quad (6)$$

At $z = H_{mono}$, the density profile $\phi(z)$ goes to zero; therefore, it makes sense to consider only the region $z \leq H_{mono}$.

Figure 1a presents the results of Monte Carlo simulation of monodisperse brushes, which are matched with formulas (3) and (4). The length of chains in monodisperse brushes is $N_n = 100$, and the grafting density is $\sigma = 0.1$, 0.2, and 0.3. For monodisperse brushes, the results of density calculations presented in Fig. 1a are well described by expression (3).

For polydisperse brushes, the density profile is determined not only by the grafting density and number-average chain length N_n but also by the chain length distribution function. If the distribution function is chosen as the Schulz–Zimm distribution, as in [36], then the profiles of brushes for various polydispersity values may be derived only numerically. In

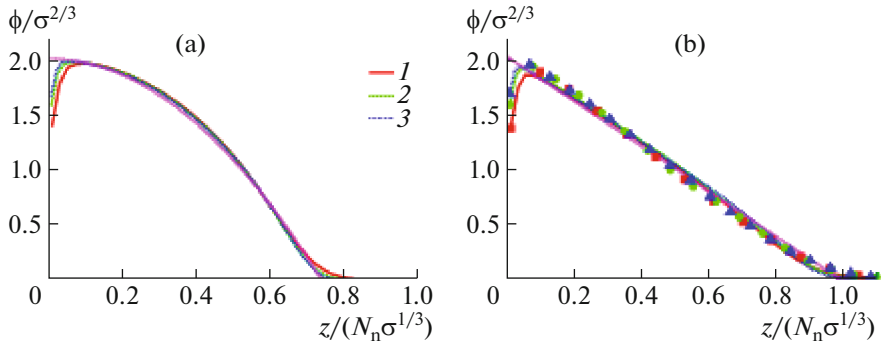

Fig. 1. (Color online) Density profiles of (a) monodisperse and (b) polydisperse brushes in a good solvent obtained by the Monte Carlo method at $N_n = 100$ and a grafting density of σ (*1*) 0.1, (*2*) 0.2, and (*3*) 0.3 in comparison with predictions from analytical theories. For polydisperse brushes, the molecular-mass distribution of chains was set as function (7) at the distribution parameter $\frac{N_w}{N_n} = 1.153$ (solid lines) and as the Schulz–Zimm distribution (1) at $\frac{N_w}{N_n} = 1.143$ (symbols). Theoretical dependences for the parabolic density profile (3) and the linear profile (8) are shown by thin lines.

[37], we managed to obtain an analytical expression for density profile using the chain length distribution in the following form:

$$P_{lin}(N) = \frac{3N}{N_{max}^2}\left(1 - \frac{N^2}{N_{max}^2}\right)^{1/2}. \quad (7)$$

This distribution is cut off at a certain maximum number of units $N_{max} = \frac{16}{3\pi}N_n$ and is characterized by the polydispersity index $N_w/N_n = 1.153$. The shape of distribution (7) is shown in Fig. 2. As is clear from

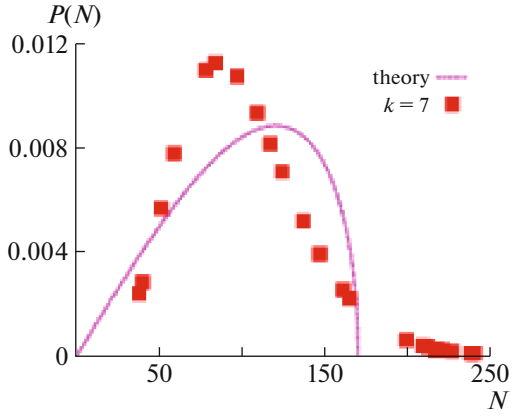

Fig. 2. (Color online) Profiles of molecular-mass distributions in polydisperse brush with the linear density profile. The solid line corresponds to the theoretical distribution (7) with $N_n = 100$ and $\frac{N_w}{N_n} = 1.153$ having the maximum value $N_{max} = 170$. Squares correspond to the Schulz–Zimm distribution (1) with N_n=100 and $\frac{N_w}{N_n} = 1.143$; $k = 7$.

formulas (6) and (7), the length distribution in the polydisperse brush has the same functional shape as the height distribution of chain ends in the monodisperse brush. As predicted by the theory [37], for this somewhat artificial shape of distribution, the density profile of the polydisperse brush should have a strictly linear shape:

$$\phi_{lin}(z) = \phi_0\left(1 - \frac{3z}{4H_{mono}}\right) = \phi_0 - fz \quad (8)$$

and the thickness of the brush is described by formula

$$H = \frac{4}{3}H_{mono}. \quad (9)$$

The self-consistent field of the brush creates the stretching force

$$f = \phi_0/H = \frac{9\pi}{16N_n}\left(\frac{\pi\sigma}{2}\right)^{1/3}, \quad (10)$$

acting on any monomer of brush chains.

Figure 1b presents the data on the Monte Carlo simulation of polydisperse brushes in comparison with predictions of the theory. The average length of chains in polydisperse brushes was the same and equal to $N_n = 100$. Grafting density σ was set to 0.1, 0.2, and 0.3.

As follows from the computer simulation of polydisperse brushes, brushes with the length distribution specified by formula (7) actually have a linear density profile at different grafting densities (Fig. 1b, solid lines). In order to clarify whether the linear density profile can be realized in the polydisperse brush at any more realistic shape of distribution, for example, at the Schulz–Zimm distribution, calculations were performed using distribution (1) at $k = 7$, which corre-

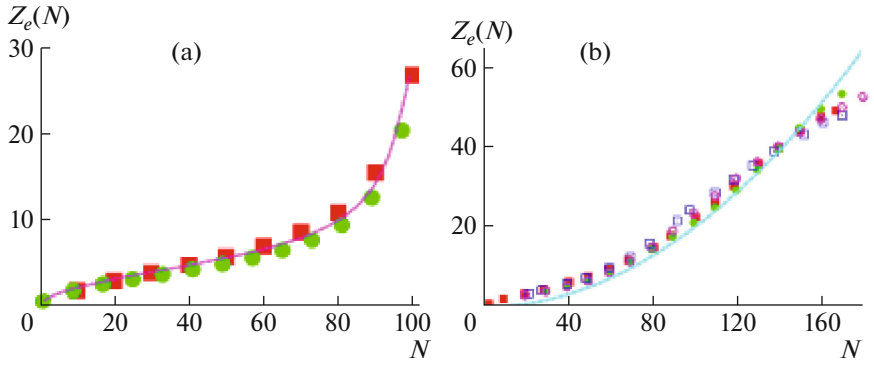

Fig. 3. (Color online) Average height of free end Z_e of probe chain as a function of its length N. Probe chains reside in (a) monodisperse brush with the squared density profile and (b) polydisperse brush with the linear density profile. The average number of minority chain units in brushes is $N_n = 100$; the grafting density is $\sigma = 0.2$. Squares and circles show the results of numerical calculations according to the self-consistent field method (circles) and Monte Carlo simulation (squares). Solid lines correspond to the analytical dependences constructed through formulas (14) and (18).

sponds to the polydispersity index $\frac{N_w}{N_n} = 1 + \frac{1}{k} \approx 1.143$. The results of calculations for different grafting densities are shown by circles, triangles, and squares in Fig. 1b. As is seen, the density profile for these brushes is also almost linear, although the shape of the chain length distribution is appreciably different (Fig. 2).

Conformations of a Probe Chain inside Monodisperse and Polydisperse Brushes

To better appreciate the difference in self-consistent fields created inside monodisperse and polydisperse brushes, let us consider first the characteristics of probe chains with length N embedded in a monodisperse brush. For a chain residing in a monodisperse brush in a good solvent, Green's function $G(z,s)$ is a solution of the Edwards equation in the presence of the parabolic potential $\omega(z)$ and provided that boundary conditions are specified as the impenetrable inert grafting plane:

$$\frac{\partial G(z,s)}{\partial s} = \frac{1}{6}\frac{\partial^2 G(z,s)}{\partial z^2} - \omega(z)G(z,s) \qquad (11)$$
$$N \geq s \geq 0$$

$$\omega(z) = \phi_0 - \frac{3\pi^2}{8}\frac{z^2}{N_n^2} = \phi(z). \qquad (12)$$

The solution takes the form [43]

$$G(z,N) = Bz\exp\left[-\frac{3\pi}{4N_n}z^2\cot\left(\frac{\pi N}{2N_n}\right)\right], \qquad (13)$$

where B is the normalization factor. If probe chains are shorter than minority chains $N \leq N_n$, then the average height of their free end $Z_e(N)$ is described by the expression

$$Z_e(N) = \left[\frac{N_n}{3}\tan\left(\frac{\pi N}{2N_n}\right)\right]^{1/2} \qquad (14)$$
$$\approx \begin{cases} (\pi N/6)^{1/2} & N \ll N_n \\ \left(\dfrac{2N_n}{3\pi(1-N/N_n)}\right) & (1-N/N_n) \ll 1 \end{cases}.$$

Figure 3a shows the average height of the free end for probe chains of different length N inside the monodisperse brush with $N_n = 100$. As is seen, analytical expressions (14) are verified by numerical calculations and simulation results. Short probe chains included in the monodisperse brush are weakly deformed coils, which begin to unwind and behave as minority chains of the brush only at N close to N_n. Folding of the probe chain to a coil proceeds if its length N is shorter than the length of minority chains by only several units, and this effect becomes more pronounced with lengthening of minority chains of the brush. It is reasonable to suggest that the monodisperse brush is characterized by a peculiar instability, because small changes in the length of any chain lead to its "falling out" from the self-consistent parabolic field of the brush.

Let us consider the polydisperse brush. In this case, it makes no sense to suggest probe chains of another length, because chains in the brush are distributed over length and are present in the self-consistent field with the linear potential $\omega(z) = -fz$. For a chain in this field, the Green's function is also the solution of the Edwards equation [44]:

$$G(z,N) = \left(\frac{2\pi N}{3}\right)^{-1/2}\exp\left[\frac{f^2N^3}{18} - \frac{3}{2N}\left(z - \frac{fN^2}{6}\right)^2\right], \qquad (15)$$

$$f = \frac{9\pi}{16N_n}\left(\frac{\pi\sigma}{2}\right)^{1/3}. \qquad (16)$$

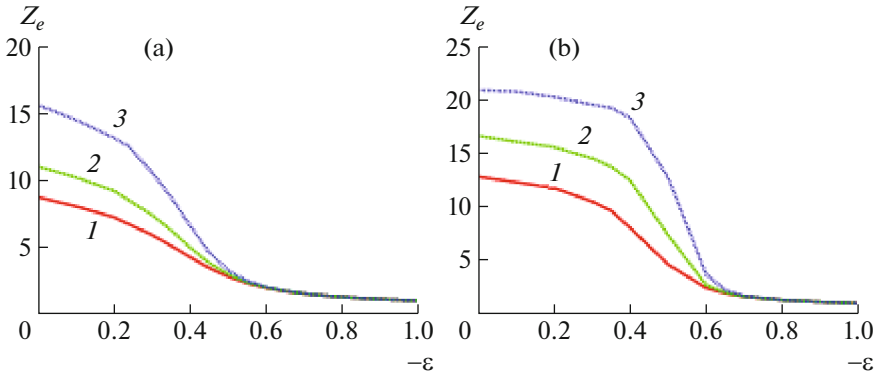

Fig. 4. (Color online) Average height of the free end Z_e of the sorption-active probe chain with length N as a function of adsorption energy of unit (−ε) in (a) monodisperse brush with the squared density profile and (b) polydisperse brush with the linear density profile. The average number of minority chain units in brushes is N_n =100; the grafting density is σ = 0.2. N = (*1*) 70, (*2*) 80, and (*3*) 90. The results are obtained by numerical calculations according to the self-consistent field method; k = 7.

If the impenetrable inert grafting plane is present, the Green's function of the chain in the polydisperse brush becomes [37]

$$G(z,N) = B'z\exp\left[-\frac{3}{2N}\left(z-\frac{fN^2}{6}\right)^2\right] \qquad (17)$$

(B' is the normalization factor, and $z \le H$).

The average height of the free end of the chain in the polydisperse brush with the linear density profile at $N \le N_n$ is described by the simple expression

$$Z_e(N) = \frac{N^2 f}{6}. \qquad (18)$$

The average height of the free end for chains of different length N inside the polydisperse brush with the linear density profile is presented in Fig. 3b. Polydisperse brushes were calculated using the chain length distribution set by formula (7) with N_w/N_n = 1.153 and the Schulz–Zimm distribution given by formula (1) at N_w/N_n = 1.143. The grafting density of brushes σ was set to be the same and equal to 0.2. The average length of minority chains N_n of brushes was also the same and equal to 100. Numerical self-consistent field calculations and Monte Carlo simulations are shown by different colored figures. Solid lines correspond to analytical dependence (18). As is seen, in the polydisperse brush, all chains are stretched and the height of their free ends always grows is proportion to the square of their contour length.

ADSORPTION TRANSITIONS OF PROBE CHAINS INSIDE BRUSHES

In this section, we will consider probe chains which have the same length as the minority chains of the brush but have another chemical nature. Another chemical nature of the probe chain will manifest itself only in relation to one parameter, namely, interaction with the solid substrate, that is, the grafting plane. If minority chains of the brush sterically repulse from the substrate, the probe chain will be capable of sorption activity. In other words, we will consider that the probe chain is adsorbed on the grafting plane, but upon addition of the desorbing agent to solution, it may desorb and switch to the exposed state, in which the minority chains of the brush occur (it is assumed that addition of the desorbing agent has no effect on properties of minority chains of the brush). The possibility of practical implementation of this system will be discussed later.

Figure 4 shows dependences of $Z_e(-\varepsilon)$ of the average height of the free ends of probe sorption-active chains residing inside monodisperse and polydisperse brushes on the energy of adsorption of the unit (−ε). The results are obtained by the numerical self-consistent field method at the same grafting density σ = 0.2 in all of the brushes and at the same value of N_n = 100. The monodisperse brush had a parabolic density profile, while for the polydisperse brush the density profile was linear. The number of units in probe chains was varied within 70–90. As is clear from Fig. 4, $Z_e(-\varepsilon)$ plots for monodisperse and polydisperse brushes are similar: in both cases, as the energy of adsorption interactions decreases, the height of chain free ends grows. This is evidence that the chains desorb and stretch along the normal to the grafting plane. The profiles of transitions are sharper for chains in the polydisperse brush. This is natural, because in this case chains are more strongly stretched in the nonadsorbed state.

Although dependences $Z_e(-\varepsilon)$ look similar for monodisperse and polydisperse brushes, the end height distributions of probe chains with N = 80 inside these brushes are substantially different (Fig. 5). In the monodisperse brush, the end height distributions are always unimodal, while in the polydisperse brush they are bimodal in the vicinity of transition. This fact indi-

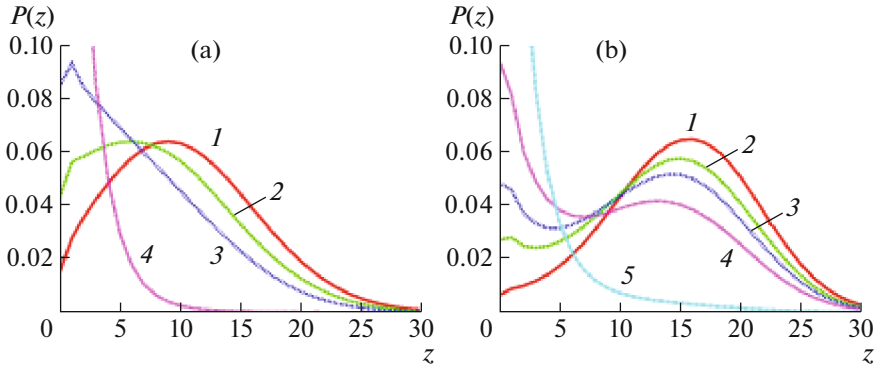

Fig. 5. (Color online) Free end height distribution of the sorption-active probe chain with length $N = 80$ at several energies of adsorption interactions. The probe chain resides inside (a) the monodisperse brush with the parabolic density profile and (b) the polydisperse brush with the linear density profile. Minority chains of brushes are sorption inactive and exist in the desorbed exposed state. The average number of minority chain units in brushes N_n is the same and equal to 100; the grafting density σ is also the same and equal to 0.2; $k = 7$; ε = (a) (*1*) 0, (*2*) −0.20, (*3*) −0.30, (*4*) −0.60 and (b) (*1*) −0.20, (*2*) −0.35, (*3*) −0.40, (*4*) −0.45, and (*5*) −0.60.

cates that, in the monodisperse brush, probe chains are adsorbed via continuous transition, whereas in the polydisperse brush the adsorption of probe chains proceeds according to the two-state principle. The adsorbed state is characterized by a narrow distribution $P(z)$ at a small height Z_e. The exposed state has a wide distribution at high values of Z_e. In the vicinity of transition, these states coexist. As is known, the picture of bimodal distributions is inherent in first-order phase transitions in finite systems [45, 46].

Analytical Description of Probe Chain Adsorption in a Polydisperse Brush

We will describe the switching transition of the sorption-active probe chain occurring inside the polydisperse chain with the linear density profile using the continuous ideal chain model. Gaussian conformations of the probe chain are disturbed under the action of the self-consistent field of the polydisperse brush $V_{brush}(z) = \phi_0 - fz$ and the adsorption interaction $V_{ads}(z)$ of the chain with the surface of grafting. In the continuous chain model, adsorption interactions between chain units and grafting plane are usually described by pseudopotential $V_{ads}(z) = -c\delta(z)$, where c is the parameter of adsorption interactions. This parameter was introduced by de Gennes to replace the real adsorption potential with the boundary condition in the Edwards equation

$$\left.\frac{\partial \ln G(z,s)}{\partial z}\right|_{z=0} = -c, \qquad (19)$$

where $N \geq s \geq 0$.

Therefore, the Edwards equation

$$\frac{\partial G(z,s)}{\partial s} = \frac{1}{6}\frac{\partial^2 G(z,s)}{\partial z^2} - V(z)G(z,s) + \delta(s)\delta(z) \qquad (20)$$

with initial conditions $G(z,0) = \delta(z)$ and boundary conditions $V(0) = V_{brush}(0) + V_{ads}(0) = \phi_0 - c$ and $V(H) = V_{brush}(H) + V_{ads}(H) = 0$ may be solved analytically and the Green's function in the adsorbed state may be written as

$$G_{ads}(z,N) = 2c\exp\left[N\left(-\phi_0 - \frac{c^2}{6}\right) - cz\right]. \qquad (21)$$

Hence, after integration over z, we arrive at the statistical sum of the probe chain in the adsorbed state:

$$Q_{ads}(N) = 2\exp\left(-N\phi_0 + N\frac{c^2}{6}\right). \qquad (22)$$

Thus, the chemical potential $\mu_{ads} = c^2/6$ has the sense of a gain in the free energy of adsorption per unit of an asymptotically long chain.

For the desorbed exposed state of the probe chain having no contacts with the grafting surface, the Green's function is given by Eq. (17). Using this expression, we may obtain the statistical sum of the probe chain in the exposed desorbed state:

$$Q_{exp} \approx BH\exp\left(-N\phi_0 + \frac{f^2N^3}{18}\right). \qquad (23)$$

Determining the transition point from the exposed state to the adsorbed one from condition $Q_{ads} = Q_{exp}$ and disregarding logarithmic corrections, we obtain

$$c_{tr} = \frac{fN}{3}. \qquad (24)$$

In accordance with Eq. (24), for adsorption of the long probe chain, a much stronger adsorption interaction of the unit with the substrate than for the short chain should be specified. Accordingly, upon addition of the desorbing agent to solution, long probe chains

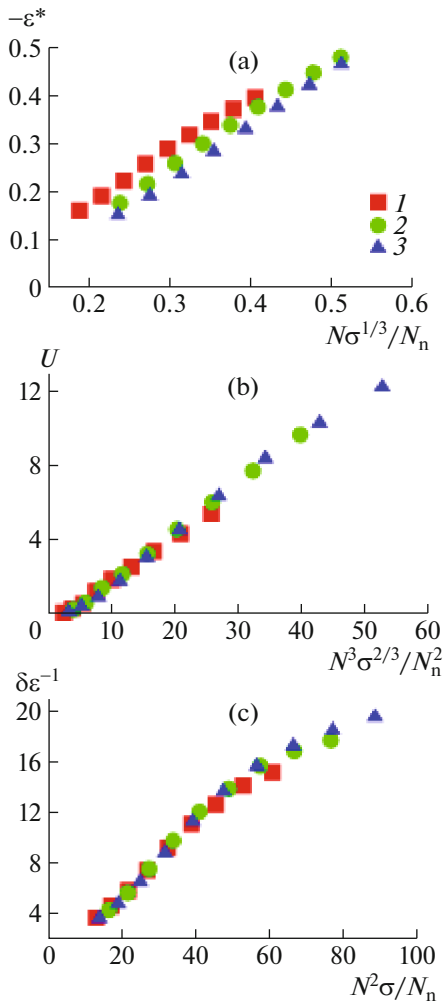

Fig. 6. (Color online) Scaling dependences of (a) the position of transition center, (b) the sharpness of transition, and (c) the height of barrier at the center of transition between exposed and adsorbed states of probe sorption-active chain inside the polydisperse brush with the linear density profile. Calculations are performed according to the self-consistent field method at a grafting density of $\sigma =$ (*1*) 0.1, (*2*) 0.2, and (*3*) 0.3; $k = 7$. The average length of probe chains in brushes is varied in the interval $N = 70, 80, \ldots, 170$. The average number of minority chain units is $N_n = 100$.

will desorb first and only then will short probe chains do so.

Remember that the adsorption of plane-grafted ideal isolated continuous model chain (in the absence of brush) takes place via a second-order phase transition at $c_{cr} = 0$. If a constant tearing force acting along the normal to the plane is applied to the end of this chain, then switching to the adsorbed state proceeds via a first-order phase transition and the value of c_{tr} equal to the value of the tearing force regardless of the chain length corresponds to the transition point [46]. Thus, action of the tearing self-consistent field of the polydisperse brush on the probe chain is dramatically different from tearing off the adsorbed chain end.

In addition to continuous chain models adsorption theories frequently use lattice models in which the energy of adsorption ($-\varepsilon$) is set in the explicit form as the depth of potential of chain interaction with the surface. In the lattice model, adsorption of the ideal isolated chain (in the absence of external forces or fields) proceeds via a second-order phase transition at the critical adsorption energy ε_c, and the chemical potential of the unit in the vicinity of transition is expressed as

$$\mu(\varepsilon) = \alpha(\varepsilon - \varepsilon_c)^2, \qquad (25)$$

where α and ε_c are model-dependent constants [46]. Comparing μ_{ads} and $\mu(\varepsilon)$ makes it possible to unveil the relation $c_{tr} \approx \varepsilon_{tr} - \varepsilon_c$ between the critical adsorption pseudopotential and lattice potential depth ($-\varepsilon_{tr}$) in describing adsorption of the ideal probe chain within the self-consistent field of the polydisperse brush and to get

$$-\varepsilon_{tr} \sim \frac{N}{N_{max}}\sigma^{1/3}. \qquad (26)$$

The sharpness of chain switching from the adsorbed state to the exposed one may be calculated through the formula obtained for the two-state model [47]:

$$(\delta\varepsilon)^{-1} = \left(\frac{1}{4}\frac{d\ln Q_{ads}}{d\varepsilon}\right)_{\varepsilon=\varepsilon_c} \sim \left(\frac{N^2}{N_{max}}\right)\sigma^{1/3}. \qquad (27)$$

As was mentioned above, the function of minority chain end height distribution is bimodal in the vicinity of transition. This finding suggests that the two mentioned states are separated by a barrier. The height of the barrier may be estimated under the assumption that, in the exposed state at $Z_e = \langle Z_e\rangle$, the chain resides at a minimum, while at $Z_e \approx \langle Z_e\rangle/2$ it occurs at the barrier apex:

$$U_{barrier} = \ln\left(\frac{G_{exp}(\langle Z_e\rangle)}{G_{exp}(\langle Z_e\rangle/2)}\right) \sim f^2N^3 \sim \frac{N^3}{N_{max}^2}\sigma^{2/3} \qquad (28)$$

The scaling dependences (26)–(28) were verified through calculation of the transition point, the sharpness of transition, and the height of barrier for probe sorption-active chains of different lengths $N = 70, 80, \ldots, 170$ inside the polydisperse brush with the linear density profile at $\sigma = 0.2$ and $N_n = 100$. The linear profile of the brush was set by the length distribution of brush minority chains as the Schulz–Zimm distribution with $k = 7$ ($N_w/N_n = 1.143$). Calculations performed by the self-consistent field method (Fig. 6) confirm the general pattern of dependences (26)–(28).

CONCLUSIONS

Hence, according to the analytical theory and computer simulation, polydisperse brushes with the Schulz–Zimm distribution at polydispersity index $N_w/N_n = 1.143$ have an almost linear density profile and form within the brush a self-consistent field, the potential of which provides the constant stretching force acting on all units of brush chains. It is interesting that, two and a half decades ago, F. Brochard-Wyart [48, 49] showed that, if a fixed-end macromolecule is imposed by a liquid flow with a constant rate, then provided that the draining is complete a constant stretching force acts on each macromolecular unit. The characteristic features of chain conformation and its normal modes in this flow were described [50]. Because the analogous conformations are realized in polydisperse brushes with a linear density profile, it would be useful to verify predictions of the theory via molecular or Brownian dynamics simulation of polydisperse brushes. Note that there is also a certain analogy between chain conformations in the monodisperse brush and the behavior of a separate macromolecule in the longitudinal hydrodynamic flow at the critical gradient [51].

Unexpected features are exhibited by the conformation discontinuous transition of the sorption-active probe chain occurring inside the polydisperse brush. It was found that, for this transition from the adsorbed state to the exposed desorbed one to occur, the value of adsorption interactions should be set different depending on probe chain length. Accordingly, at the same fixed level of adsorption interactions of probe chain unit with the substrate, short probe chains may reside in the adsorbed state, whereas long chains turn out be desorbed. Naturally, this is associated with the effect of the self-consistent field of the polydisperse brush; the higher the chain parts from the planar grafting surface, the stronger the field stretches them. In the analytical theory, we took into account the effect of self-consistent field of the brush only on the completely exposed desorbed state assuming that the adsorbed state is determined only by the energy of adsorption interactions of probe chain units with the grafting surface. However, the stretching field of the brush evidently acts on all fragments of the probe adsorbed chain unbound to the surface—its ends and loops. Taking into account these interactions, which may be substantial in the description of adsorption of probe chains at low adsorption energies, is a separate task.

Now we touch on two questions which were asked in various auditoria when discussing this work. Why do short probe chains in the monodisperse brush switch to the adsorbed state via the continuous diffuse pathway, while in the polydisperse brush this transition is sharp? To answer this question it is best to discuss the limiting case of the Alexander brush with the density profile as a step. In this stepwise potential, a short probe chain "does not know" that the field formed by the brush somewhere goes to zero and, therefore, assumes the conformation of a chaotically folded coil. The transition of the coil to the adsorbed state is known to proceed smoothly without jumps. The density profile of the monodisperse brush looks like a step; therefore, the adsorption of short chains in the monodisperse brush also looks like a continuous transition. In addition, in the polydisperse brush with a linear density profile, even short probe chains are stretched by the brush field. As a result, switching of the stretched chain to the adsorbed state proceeds sharply via overcoming of the barrier.

The second question is related to difference of the probe chain, which is supposed to be sorption active, from minority chains of the brush inert with respect to the grafting surface. According to the theory, the chemical structure of the probe chain is different from the chemical structure of minority chains of the brush; however, it is assumed that the thermodynamic flexibility of both types of chains is the same or at least similar. It is also supposed that interaction of these two types of chains with the solvent is also the same—the solvent is assumed to be good in all of the cases. The question arises to what extent this situation is realistic and whether these chemically different chains (probe chain and minority chains of the brush) exist, which under the same conditions (in the same solvent and at the same temperature) demonstrate a sharp difference only with respect to their sorption activity.

Needless to say, not any pair of chemically different chains under the same conditions is distinguished solely by sorption activity. However, these pairs do exist, especially in mixed solvents, for example, poly(methyl methacrylate) and polystyrene in methyl ethyl ketone–cyclohexane mixture taken at a volume ratio of 86 : 14. This solvent is good for both polymers. Note that the first polymer with a change in the composition of the solvent switches to the adsorbed state, whereas the second one remains sorption inactive [52]. A similar behavior of this pair of polymers is observed in CH_2Cl_2/CH_3CN mixture (74 : 26, vol/vol) [53]. Mixed solvents specially selected for polystyrene and polybutadiene, poly(ethylene glycol) and poly(propylene glycol), and other pairs are given in book [54].

In conclusion, let us dwell on some features of the adsorption transition of the probe chain residing inside the polydisperse brush and its difference from other adsorption transitions. As was mentioned above, adsorption of the grafted isolated chains (in the absence of brush), provided that a constant tearing force is applied to the chain end along the normal to the plane, proceeds discontinuously [46]. The transition point, that is, the energy of adsorption required for transition from the exposed state to the adsorbed one, is independent of chain length and is determined solely by the applied stretching force. This discontinu-

ous transition from the exposed state to the adsorbed one has unusual features typical of second-order transitions. Namely, throughout the transition region, the distribution over the order parameter (over free end height) remains unimodal, and fluctuations in the vicinity of the transition point grow according to a power law. Recent studies showed [55] that, in the vicinity of transition, there is a critical retardation of order parameter relaxation times typical of critical phenomena. Thus, in the adsorption of end-stretched chain, features of first- and second-order phase transitions manifest themselves. The reasons behind this phenomenon are associated with the microphase state of the system and are discussed in [56].

Adsorption of the probe chain in the self-consistent field of the polydisperse brush likewise occurs discontinuously but with the bimodal distribution over the order parameter (over free end height), in accordance with the standard classification of first-order phase transitions. However, this transition demonstrates unusual features: the transition point, that is, the energy of adsorption corresponding to the midpoint of transition, is proportional to the contour length of the adsorbing chain N, the sharpness of transition is proportional to N^2, and the height of barrier separating adsorbed and desorbed states is proportional to N^3. To our knowledge, the specific system demonstrating these features of the first-order phase transition was reported for the first time.

ACKNOWLEDGMENTS

This work was supported by the Netherlands Organisation for Scientific Research–Russian Foundation for Basic Research, grant 17-53-12013NNIO-a.

REFERENCES

1. N. Ayres, Polym. Chem. **1**, 769 (2010).
2. G. D. Bixler and B. Bhushan, Philos. Trans. R. Soc., A **370**, 2381 (2012).
3. B. Zdyrko, V. Klep, X. Li, Q. Kang, S. Minko, X. Wen, and I. Luzinov, Mater. Sci. Eng., A **29**, 680 (2009).
4. J. Klein, D. Perahia, and S. Warburg, Nature **352**, 143 (1991).
5. M. K. Singh, P. Ilg, R. M. Espinosa-Marzal, M. Kroger, and N. D. Spencer, Langmuir **31**, 4805 (2015).
6. J. Klein, Science **323**, 47 (2009).
7. StuartM. A. Cohen, W. T. S. Huck, J. Genzer, M. Muller, C. Ober, M. Stamm, G. B. Sukhorukov, I. Scleifer, V. V. Tsukruk, M. Urban, F. Winnik, S. Zauscher, L. Lusinov, and S. Minko, Nat. Matter **9**, 101 (2010).
8. *Handbook of Stimuli-Responsive Materials,* Ed. by U. U. Marek (Wiley-VCH Verlag GmbH and Co. KGaA, Weinheim, 2011).
9. W. L. Chen, R. Cordero, H. Tran, and C. K. Ober, Macromolecules **50**, 4089 (2017).
10. S. Alexander, J. Phys. (Paris) **38**, 977 (1977).
11. A. A. Gorbunov, I. V. Pavlushkov, and A. M. Skvortsov, Vysokomol. Soedin., Ser. A **30** (2), 431 (1988).
12. A. M. Skvortsov, I. V. Pavlushkov, and A. A. Gorbunov, Vysokomol. Soedin., Ser. A **30** (4), 503 (1988).
13. A. M. Skvortsov, I. V. Pavlushkov, A. A. Gorbunov, E. B. Zhulina, O. V. Borisov, and V. A. Pryamitsyn, Vysokomol. Soedin., Ser. A **30** (8), 615 (1988).
14. E. B. Zhulina, V. A. Pryamitsyn, and O. V. Borisov, Vysokomol. Soedin., Ser. A **31** (1), 185 (1989).
15. S. T. Milner, T. A. Witten, and M. Cates, Europhys. Lett. **5**, 413 (1988).
16. S. T. Milner, T. A. Witten, and M. Cates, Macromolecules **21**, 2610 (1988).
17. S. Hirz, Masters Thesis (Univ. Minnesota, 1986).
18. S. T. Milner, Science **251**, 905 (1991).
19. S. T. Milner, T. A. Witten, and M. Cates, Macromolecules **22**, 853 (1989).
20. G. J. Fleer, M. A. Cohen-Stuart, J. M. H. M. Scheutjens, T. Cosgrove, and B. Vinsent, in *Polymer at Interfaces* (Chapman and Hall, London, 1993).
21. E. B. Zhulina, O. V. Borisov, V. A. Pryamitsyn, and T. M. Birshtein, Macromolecules **24**, 140 (1991).
22. T. M. Birshtein and V. M. Amoskov, Polym. Sci., Ser. C **42** (1), 172 (2000).
23. K. Binder and A. Milchev, J. Polym. Sci., Polym. Phys. Ed. **50**, 1515 (2012).
24. E. B. Zhulina, O. V. Borisov, and L. Brombacher, Macromolecules **24**, 4679 (1991).
25. C. M. Wijmans, E. B. Zhulina, and G. J. Fleer, Macromolecules **27**, 3238 (1991).
26. T. Kreer and S. M. Balko, ACS Macro Lett. **2**, 944 (2013).
27. J. I. Martin and Z. G. Wang, J. Phys. Chem. **99**, 2833 (1995).
28. T. Kreer, Soft Matter **12**, 3479 (2016).
29. A. A. Polotsky, F. A. M. Leermakers, E. B. Zhulina, and T. M. Birshtein, Macromolecules **45**, 7260 (2012).
30. A. A. Polotsky, A. D. Kazakov, and T. M. Birshtein, Polymer **130**, 242 (2017).
31. A. M. Laradji, C. D. McNitt, N. S. Yadavalli, V. V. Popik, and S. Minko, Macromolecules **49**, 7625 (2016).
32. C. S. Turgman, J. Srogl, D. Kiserow, and J. Genzer, Langmuir **31**, 2372 (2015).
33. B. M. Berg, H. Vink, and J. A. E. Spaan, Circ. Res. **92**, 592 (2003).
34. S. T. Milner, Europhys. Lett. **7**, 695 (1988).
35. S. Milner, T. Witten, and M. Cates, Macromolecules **22**, 853 (1989).
36. W. M. de Vos and F. A. M. Leermakers, Polymer **50**, 305 (2009).
37. QiS. Shuanhu, L. I. Klushin, A. M. Skvortsov, and F. Schmid, Macromolecules **49**, 9665 (2016).
38. L. I. Klushin, A. M. Skvortsov, A. A. Polotsky, Qi S. Shuanhu, and F. Schmid, Phys. Rev. Lett. **113**, 068303 (2014).
39. M. Laradji, H. Guo, and M. J. Zuckermann, Phys. Rev. E: Stat. Phys., Plasma, Fluids, Relat. Interdiscip. Top. **49**, 3199 (1994).

40. Qi S. Shuanhu, L. I. Klushin, A. M. Skvortsov, A. A. Polotsky, and F. Schmid, Macromolecules **48**, 3775 (2015).
41. G. V. Schulz, Z. Phys. Chem. (Meunchen, Ger.) **43**, 25 (1939).
42. B. Zimm, J. Chem. Phys. **16**, 1099 (1948).
43. A. M. Skvortsov, A. A. Gorbunov, and L. I. Klushin, Macromolecules **30**, 1818 (1997).
44. M. L. Mansfield, J. Chem. Phys. **88**, 6570 (1988).
45. A. M. Skvortsov, L. I. Klushin, and T. M. Birshtein, Polym. Sci., Ser. A **51** (5), 469 (2009).
46. L. I. Klushin and A. M. Skvortsov, J. Phys. A: Math. Theor. **44**, 473001 (2011).
47. M. Challa, D. Landau, and K. Binder, Phase Transform. **24–26**, 343 (1990).
48. F. Brochard-Wyart, Europhys. Lett. **23**, 105 (1993).
49. F. Brochard-Wyart, Europhys. Lett. **30**, 387 (1995).
50. Y. Marciano and F. Brochard-Wyart, Macromolecules **28**, 985 (1995).
51. L. I. Klushin and A. M. Skvortsov, Vysokomol. Soedin., Ser. A **32** (8) (1990).
52. H. Gao, K. Min, and K. Matyjaszewski, Macromol. Chem. Phys. **207**, 1709 (2006).
53. T. Chang, J. Polym. Sci., Polym. Phys. Ed. **43**, 1591 (2005).
54. H. Pasch and B. Trathnigg, in *Multidimensional HPLC of Polymers* (Springer, New York, 2013).
55. S. Zhang, S. Qi, L. I. Klushin, A. M. Skvortsov, D. Yan, and F. Schmid, J. Chem. Phys. **147**, 064902 (2017).
56. A. M. Skvortsov, L. I. Klushin, A. A. Polotsky, and K. Binder, Phys. Rev. E: Stat., Nonlinear, Soft Matter Phys. **85**, 031803 (2012).

Translated by T. Soboleva